Mechanical Properties of Epoxy Networks Based on DGEBA and Aliphatic Amines

Filiberto González Garcia,[1,2] **Bluma G. Soares,**[2] **Victor J. R. R. Pita,**[2]
Rubén Sánchez,[3] **Jacques Rieumont**[4]

[1]*Departamento Materiais, Instituto Politécnico, Universidade do Estado do Rio de Janeiro, Rua Alberto Rangel s/n, Vila Nova, 28630-050, Nova Friburgo, RJ, Brazil*
[2]*Instituto de Macromoléculas, Universidade Federal do Rio de Janeiro, Centro de Tecnologia, Bl J, Ilha do Fundão, 21945-970, Rio de Janeiro, RJ, Brazil*
[3]*Laboratório de Materiais Avançados–LAMAV, Universidade Estadual do Norte Fluminense, Centro de Ciências e Tecnologia, Ave. Alberto Lamego, 2000, 28015-620 Campos dos Goytacazes, RJ, Brazil*
[4]*Facultad de Química, Universidade de La Habana, Ave. Zapata y G, La Habana 10400, Cuba*

ABSTRACT: The mechanical properties of epoxy networks based on diglycidyl ether of bisphenol A epoxy resin cured with various linear aliphatic amines, such as ethylenediamine, diethylenetriamine, triethylenetetramine, tetraethylenepentamine, and cyclic amines such as 1-(2-aminoethyl)-piperazine and isophorone diamine, were studied. General characteristics such as T_g, density, and packing density, were determined and related to the structure and funcionality of the curing agent. Dynamic mechanical spectra were used to study both the α and β relaxations. Tensile and the flexural tests were used to determine the Young's and flexural modulus, and fracture strength all in the glassy state. Furthermore, linear elastic fracture mechanics was used to determine K_{IC}. As a rule, isophorone diamine network presented the higher tensile and flexure modulus while 1-(2-aminoethyl)piperazine gave the highest toughness properties. © 2007 Wiley Periodicals, Inc. J Appl Polym Sci 106: 2047–2055, 2007

Key words: epoxy resin; aliphatic amine; network; mechanical properties

INTRODUCTION

Epoxy resins are some of the most important thermosetting polymers and have wide use as structural adhesives and matrix resins for fiber composites, but their cured resins have a drawback, being brittle and having poor resistance to crack propagation. The toughness of epoxy resins has been increased by blending with reactive liquid rubbers such as carboxyl-terminated butadiene-acrylonitrile rubbers[1,2] or terminally functionalized engineering thermoplastics.[3,4] The toughness results from separation of a randomly dispersed rubbery or engineering phase in the epoxy resin during cure. Another possible way of toughening epoxy networks is to act on the structure of the epoxy resin[5–9] or on the diamine comonomer.[10–12]

The aim of this work is an attempt to evaluate the effects of the curing agent chemical structure of linear and cyclic aliphatic amines on the thermal relaxations and mechanical properties of various epoxy/aliphatic amine networks.

To maintain a high functionality a series of linear ethyleneamines were chosen. Four ethyleneamines, ethylenediamine (EDA), diethylenetriamine (DETA), triethylenetetramine (TETA), and tetraethylenepentamine (TEPA) were selected. The two other curing agents are cycloaliphatic amines based on 1-(2-aminoethyl)piperazine (AEP) and isophorone diamine (IPD), having both cyclic structures. In this case, the combination of a linear and cyclic structure in AEP imparts higher flexibility when compared with the cyclic structure in IPD.
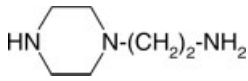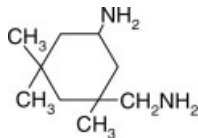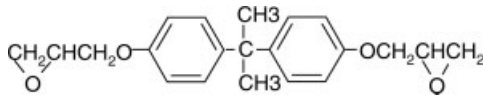
EXPERIMENTAL

Sample preparation

The formulations used in this study are based on the diglycidyl ether of bisphenol A (DGEBA) epoxy resin, Dow DER 331, cured with various aliphatic amines as comonomers: EDA, DETA, TETA, TEPA, AEP, and IPD. The formulae, suppliers, purity, molecular weight, and functionality of the various products are listed in Table I. These products are used as received. The networks were prepared by carefully

WILEY
InterScience®
DISCOVER SOMETHING GREAT

<div align="center">

TABLE I
Structure and Characteristics of the Various Monomers

</div>

Monomers	Formula	Supplier	M (g mol^{-1})	F
Ethylenediamine (EDA)	$H_2N-(CH_2)_2-NH_2$	Aldrich (99.0%)	60	4
Diethylenetriamine (DETA)	$H_2N-(CH_2)_2-NH-(CH_2)_2-NH_2$	ACROS (98.5%)	103	5
Triethylenetetramine (TETA)	$H_2N-(CH_2)_2-NH-(CH_2)_2-$ $NH-(CH_2)_2-NH_2$	Dow Chemical DEH 24	146	6
Tetraethylenepentamine (TEPA)	$H_2N-(CH_2)_2-NH-(CH_2)_2-NH-$ $(CH_2)_2-NH-(CH_2)_2-NH_2$	ACROS (Technical)	189	7
1-(2-Aminoethyl)piperazine (AEP)	HN⟨ ⟩N-(CH$_2$)$_2$-NH$_2$	ACROS (99.0%)	129	3
Isophorone diamine (IPD)	[structure]	ACROS (99+%)	170	4
Diglycidyl ether of bisphenol A (DGEBA)	[structure]	Dow Chemical DER 331	~ 374 (187g eq^{-1}*)	2

M = molecular weight, F = functionality.
* Determined by acid titration.

weighing the curing agent at the stoichiometric proportion, thoroughly mixed and cured for 24 h at room temperature. For the formulations based on TETA and TEPA curing agents corresponding to technical commercial products was necessary to determine the amine equivalent by differential scanning calorimetry to calculate the stoichiometric proportion of the amine/epoxy resin. Reaction conditions are given in "Results and Discussion section."

Determination of the packing density

The packing density at room temperature is given by:

$$\rho* = \rho\left(\frac{V_W}{M}\right) \tag{1}$$

where ρ is the density, M is the molecular weight of the constitutional repeat unit (CRU), and V_W is the Van der Waals volume of the latter. V_W is obtained by summation of the molar group contributions given by Bondi.[13] The CRU chosen is representative of the network structure, based on two molecules of DGEBA and one of amine.[14] We considered the molecular weight of epoxy resin equal to 340 g mol^{-1}.

Densities at room temperature are determined using the following empirical relationship:[15]

$$\rho = 350 + 120M\,(\text{kg m}^{-3}) \tag{2}$$

Differential scanning calorimetry

The DSC analyses were performed on a Perkin–Elmer Model DSC 7 under nitrogen purge. The epoxy/amine formulations were heated from –30 to 200°C at a rate of 10°C min^{-1}. The reaction heat ΔH was determined from the first scan. The samples were cooled at room temperature and heated again at the same rate, to obtain the glass transition temperature T_g of the fully-cured networks. The T_g is taken at the middle of the change in heat capacity (middle of transition).

Dynamic mechanical measurements

The dynamic mechanical properties of the epoxy networks were obtained using a TA Instruments DMA 2980. The samples were shaped using a silicone cavity mold yielding the specimen geometry of approximately 60 × 12.5 × 2.5 mm^3. The α transition were studied using the apparatus in double cantilever bending mode, between 30 and 180°C at a heating rate of 2°C min^{-1} and a frequency of 1 Hz. The β relaxation is
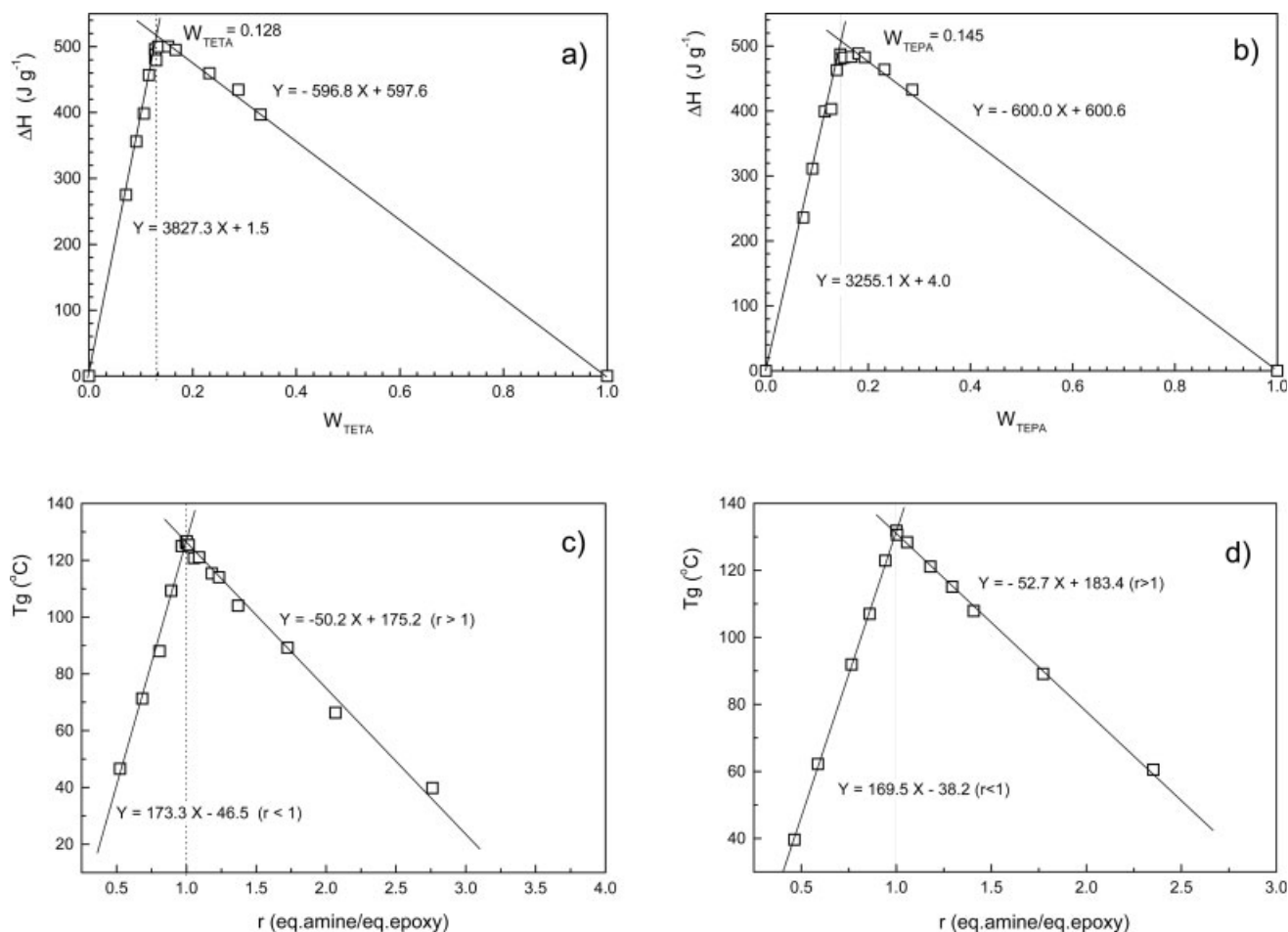
Figure 1 (a,b) Dependence of reaction heat with concentration of TETA and TEPA, respectively. (c,d) dependence of glass transition temperature with concentration of TETA and TEPA, respectively.

studied using the apparatus in double cantilever bending mode, between −120 and 40°C at a heating rate of 2°C min^{-1} in a frequency range from 3×10^{-2} to 3×10^1 Hz. The apparent activation energy $E_{a\beta}$ of the β relaxation was determined using an Arrhenius law on the maxima of the β peak (T_β).

$$\log \nu = E_{a\beta}/RT_\beta + \text{constant} \quad (3)$$

Mechanical testing

The epoxy networks were tested under flexural conditions. The mechanical tests were carried out by means of universal testing machine, model 4204, Instron. The values of flexural stress, flexural modulus, and flexural strain were determinated. All measurements were conducted in three-point bending using a crosshead speed of 10 mm min^{-1}, with length between supports equal to 50 mm and specimen dimensions equal to 3.3×12 mm cross-section and 65 mm in length according to ASTM D 790-03 protocol. Measurements were performed for each sample at $(50 \pm 5)\%$ relative humidity at (23

$\pm$ 2)°C, and the results averaged to obtain a mean value.

The samples were tested to fracture and the maximum stress (σ_y), maximum strain (ε_y), and the flexural modulus (E_y) were calculated from the following equations:

$$\sigma_y = 3PL/2bd^2 \quad (4)$$

$$\varepsilon_y = 6Dd/L^2 \quad (5)$$

$$E_y = L^3m/4bd^3 \quad (6)$$

where P is the load at the break or yield, b and d are the width and the thickness of the specimen respectively, L is the length between supports, D is the maximum deflection of the center of the beam, and m is the slope of the initial straight-line portion of the load-deflection curve.

Tensile tests were made using the same testing machine at (23 ± 2)°C and a crosshead speed of 1.0 mm min^{-1}, according to ASTM D 638. The strain is recorded by means of an axial strain gauge to measure
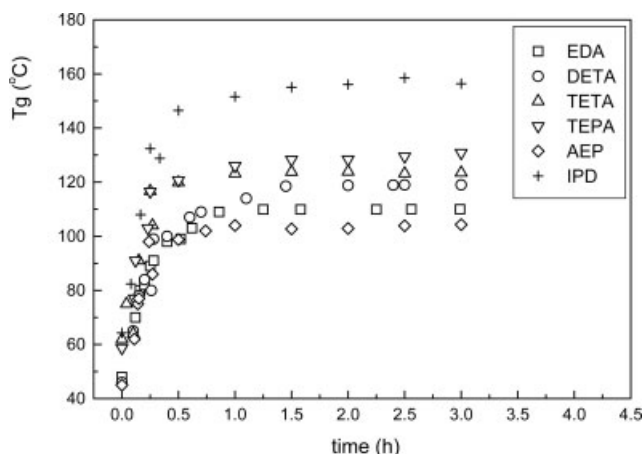
Figure 2 Glass transition temperature T_g as a function of postcure time for all the formulations studied in this work after cured 24 h at room temperature.

the axial extension upon loading. The Young's modulus E was computed from the linear part of the curve; elongation and stress at break were also recorded.

For linear elastic fracture mechanics single-edge-notched specimens (thickness = 5.25 mm, width = 10.5 mm) were used in three-point bending mode (span length = 42 mm) with a crosshead speed of 10 mm min^{-1} using the method described in ASTM D 5045. Cracks of various lengths ''a'' were machined with a saw and the crack tip was achieved with a razor blade. Four to six specimens were tested for each epoxy networks, and the fracture toughness K_{IC} was determined using the formula:

$$K_{IC} = \frac{P_{max}}{BW^{1/2}} f(a/W) \quad (7)$$

where P_{max} is the maximum load at failure, B is the sample thickness, W is the overall length, a is the

crack length and $f(a/W)$ is an expression accounting for the geometry of the sample identified in ASTM D 5045. The fracture energy G_{IC} in plane strain conditions is defined as:

$$G_{IC} = \frac{K_{IC}^2}{E}(1 - \nu^2) \quad (8)$$

where ν is the Poisson's ratio, taken to be 0.35, and E is Young's modulus.

RESULTS AND DISCUSSION

Stoichiometric proportion, curing parameters and general characterization

The formulations based on TETA and TEPA curing agents were firstly studied to investigate the stoichiometric proportion of the amine related to the epoxy resin, the reaction heat ΔH, and the glass transition temperature of the different networks (T_g) were determined as a function of the amine concentration, by using DSC analysis. According to the literature, at the stoichiometric epoxy/amine ratio, the extent of cure is expected to be maximum and, consequently, the highest value of ΔH is expected.[16–18] Beyond the stoichiometric ratio, the ΔH value decreases due to plasticization effect caused by the excess of curing agent.

Figure 1(a,b) show the experimental relationship of the reaction heat as a function of the amine concentration, for the formulations based on TETA and TEPA curing agents, respectively. The TETA formulation presented the intersection of the experimental values at $W_{TETA} = 0.128 \pm 0.01$, which corresponds to a TETA concentration of 14.7 phr (14.7 parts of TETA per 100 parts of DGEBA) and an equivalent

TABLE II
Curing Parameters and Characteristics of the Different Networks

Network	Curing cycles	Time of vitrification/cure temperature (h/°C)	T_g (°C)	ρ (g cm^{-3})	ρ*
DGEBA/EDA	24 h at *RT* ± 2 h 120°C	1.5/120	110	1.142	0.656
DGEBA/DETA	24 h at *RT* ± 2 h 120°C	1.0/120	119	1.133	0.659
DGEBA/TETA	24 h at *RT* ± 2 h 130°C	1.0/130	124	1.124	0.661
DGEBA/TEPA	24 h at *RT* ± 2 h 130°C	1.5/130	126	1.116	0.663
DGEBA/AEP	24 h at *RT* ± 2 h 120°C	1.0/120	110	1.132	0.659
DGEBA/IPD	24 h at *RT* ± 2 h 160°C	1.5/160	155	1.111	0.665

RT = room temperature, T_g = glass transition temperature, ρ = density, ρ* = packing density.
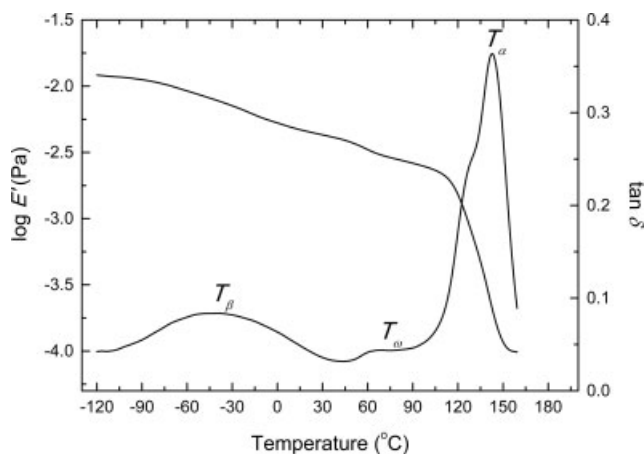
Figure 3 Dynamical mechanical properties of the DGEBA/TETA network, measured at 1 Hz.

mass of 27.5 g eq^{-1}. ΔH value at the maximum corresponds to 486 $\pm$ 10 J g^{-1} (104 kJ mol^{-1}), that lies in the range of values reported for several epoxy/amine systems.[19–21]

The intersection of the experimental values of ΔH for the TEPA formulation was found at W_{TEPA} = 0.145 $\pm$ 0.01, which corresponds to a TEPA concentration of 17.0 phr and an equivalent mass of active groups of 31.8 g eq^{-1}. The ΔH value at maximum corresponds to 490 $\pm$ 10 J g^{-1} (107 kJ mol^{-1}).

The dependence of T_g with the epoxy/amine equivalent mass ratio is illustrated in Figure 1(c,d). In both cases, the highest value of T_g was obtained at the stoichiometric proportion of hardener/epoxy system. For the formulations based on TETA and TEPA curing agents at the stoichiometric ratio T_gs were found to be 124°C and 126°C, respectively and agrees with the value reported in literature for epoxy/aliphatic amine networks.[21]
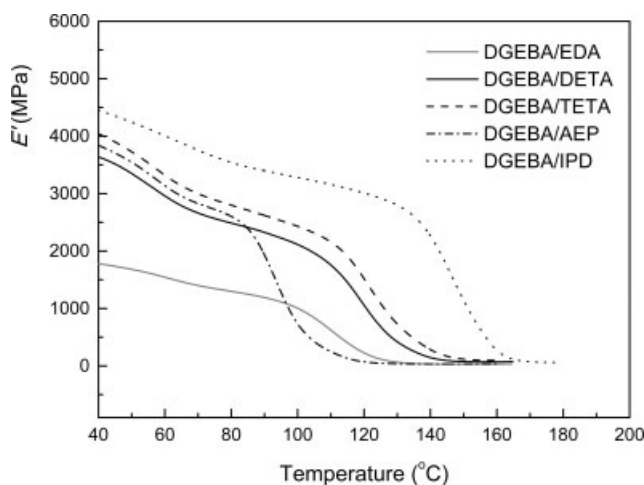
The weight fraction of TETA or TEPA was calculated according to eq. (9):

$$W_{TETA} = \frac{m_{TETA}}{m_{TETA} + m_{DGEBA}} \quad (9)$$

where m_{TETA} and m_{DGEBA} are the amine and epoxy masses introduced in the mixture.

The curing parameters of the epoxy/amine system were also studied in order to define an appropriate cure cycle. The curing schedule at room temperature for 24 h was assumed to go to completion of vitrification during this period. Accepting this is necessary to define the postcured temperature and the postcured time for all networks to obtain the highest value of T_g. For this it is necessary a higher temperature than the maximum glass transition temperature $T > T_g$.[22]

Figure 2 shows the glass transition temperature T_g as a function of postcure time for all the formulations studied in this work after curing for 24 h at room temperature. For the TETA formulation it was observed that after a reaction time of 0.75 h the T_g value is constant indicating that vitrification occurred at this polymerization temperature. The TETA formulation cured for 24 h at room temperature was postcured 2 h at 130°C. DSC scans of these samples showed a T_g = 124°C in the middle of transition and not residual reaction heat. Therefore, fully converted samples could be obtained by the selected cure schedule.

A similar procedure was carried out for the formulations based on EDA, DETA, TEPA, AEP, and IPD as curing agents. The highest value of T_g was obtained by DSC after complete cure for all the cases, the vitrification time, curing cycles, densities
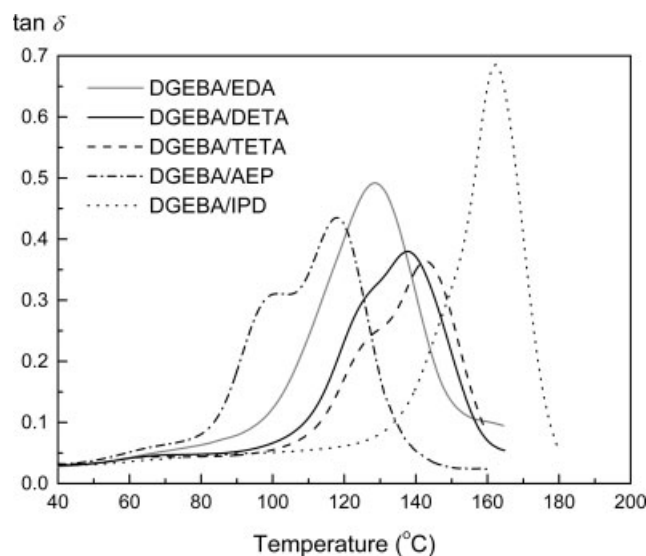

Figure 4 Modulus E' as a function of temperature at 1 Hz.

Figure 5 Tan δ as a function of temperature at 1 Hz.

TABLE III
Characteristics of the α Relaxation at 1 Hz

Networks	T_α (°C)	tan δ
DGEBA/EDA	128	0.49
DGEBA/DETA	137	0.38
DGEBA/TETA	142	0.36
DGEBA/AEP	117	0.43
DGEBA/IPD	162	0.68

T_α = temperature at the maximum, tan δ = amplitude of the loss peak at its maximum.

TABLE IV
Characteristics of the β Relaxation at 1 Hz

Networks	T_β (°C)	S_β	$E_{a\beta}$ (kJ mol^{-1})
DGEBA/EDA	−52	8.98	51
DGEBA/DETA	−43	8.76	64
DGEBA/TETA	−42	10.09	49
DGEBA/TEPA	−41	9.48	50
DGEBA/AEP	−49	8.84	52
DGEBA/IPD	−69	8.24	46

T_β = temperature at the maximum, S_β = area under the β peak, $E_{a\beta}$ = activation energy.

ρ, and the packing densities ρ* are presented in Table II.

For the series EDA-DETA-TETA-PEPA T_g increasing correlates with amine linear chain and functionality. Furthermore, T_g correlates with packing density and inversely with bulk density.

For cyclic amines (between AEP and IPD) a similar trend holds. It seems that packing density of network, related to initial functionality, is ruling the network stiffness.

Dynamic mechanical measurements

A typical plot of the storage modulus E' and tan δ, measured at 1 Hz, as a function of temperature, is shown in Figure 3 for the DGEBA/TETA network. Three relaxations are observed:

1. a main transition, α in the high-temperature region, is associated with the glass transition;
2. a secondary relaxation, β , below 0°C; and
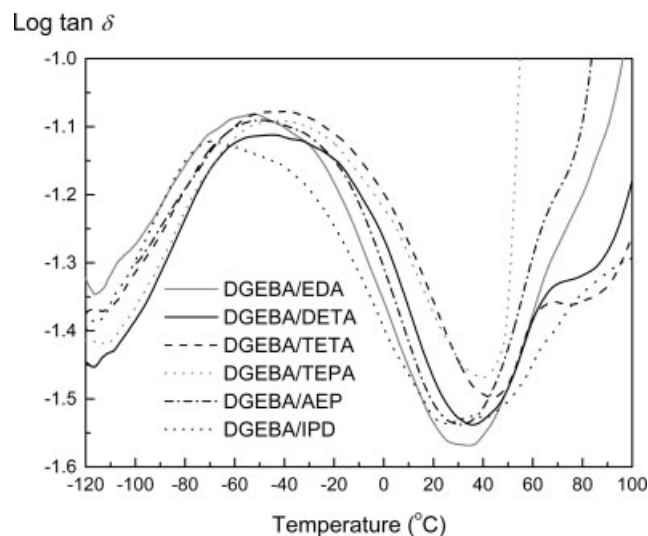3. an intermediate relaxation, ω, between 39 and 70°C

In this work, only the α and β relaxations were considered for the various networks.

Glass transition region (T_α)

The dynamic mechanical spectra for the high-temperature region are shown in Figures 4 and 5 for five networks.

Table III gives the values of the mechanical relaxation T_α determined at the maximum of the loss peak and the intensity at this maximum (tan δ).

The differences between the shapes of the α peaks are related to the structure of the hardener: The increase of functionality for the TETA compared with EDA on the series of ethyleneamines leads to an increase in T_α and a decrease in tan δ.

For cyclic curing agents a similar trend in T_α is observed but not for tan δ. This difference could be related to the fact that AEP and IPD structures are cyclic but the first one possesses a linear segment.
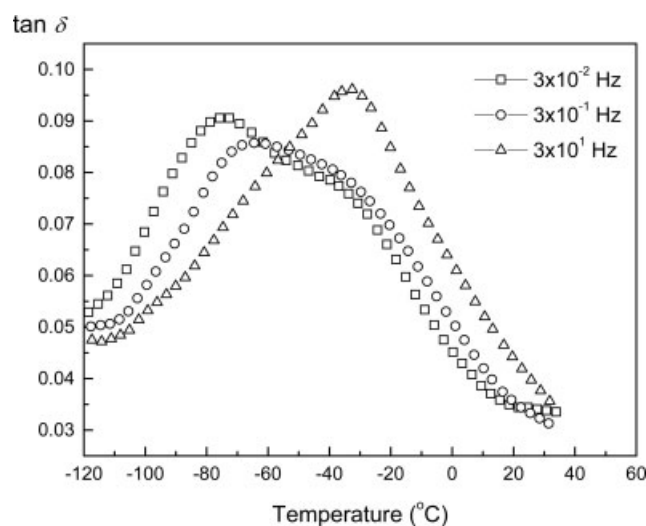

Figure 6 β Relaxation for the various networks measured at 1 Hz.

Figure 7 β Relaxation for the DGEBA/IPD network: (□) at 3×10^{-2} Hz; (○) at 3×10^{-1} Hz; (Δ) at 3×10^{1} Hz.
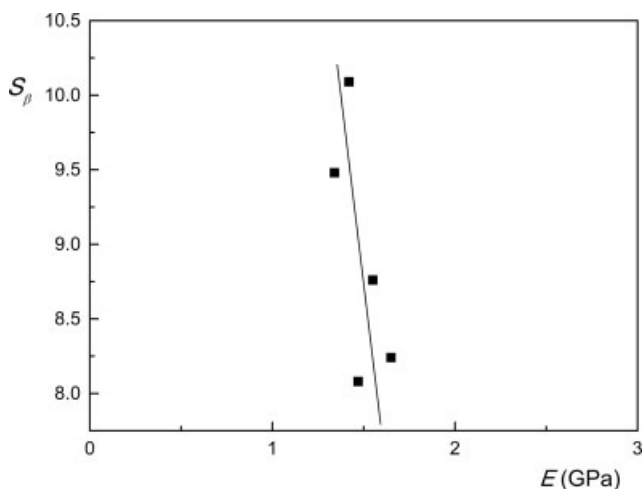
Figure 8 Area of the β relaxation as a function of Young's modulus.

The β relaxation (T_β)

The assignment of the β relaxation to short molecular segment motion depends on the chemical structure of the compounds.[23–25] For epoxy/amine networks, most authors[26–32] associate the β relaxation (between −80 and −40°C) with motion contributions of diphenylpropane groups and glyceryl units:

$$-CH_2-CH-CH_2-O-$$
$$\qquad\ \ |$$
$$\qquad\ OH$$
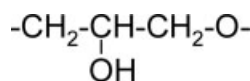
Spectra for six networks are shown in Figure 6 and their characteristics (T_β = temperature of tan δ_{max}, S_β = area under the tan δ curve) are reported in Table IV. Results presented in Table IV are not easy to rationalize.

β Relaxation in the linear series is similar for DETA, TETA, and TEPA in spite of different functionality. However, EDA, the shortest curing agent, gives a less rigid local motion (T_β = −52). But no correlation is observed for S_β or $E_{a\beta}$. It has been suggested that the $E_{a\beta}$ value decreases with increasing molecular weight of segment between crosslinked points of the curing agent.[33] For the linear series this segment is the same, thus, it is to be expected the same value of $E_{a\beta}$. These values are similar except for the DETA network.

These results are indicating that some relaxation mechanisms due to hydroxy ether,[30,32,34] diphenyl propane[32] and crosslinking[35] are operating in some extent but in a complex way. In Figure 6 the smooth curves seem to indicate that the three possible groups contributions are coupled.

For the cyclic amines observed results in Table IV are more uniform. $E_{a\beta}$ is in line with T_β because rotational barriers should operate in the same way, thus, β relaxation, S_β and $E_{a\beta}$ present the same decreasing trend from AEP to IPD. The IPD network shows the lesser T_β, possibly due to a more free cycle relaxation. For this network was observed a particular and interesting trend at different frequencies (Fig. 7). At low frequency the plot of tan δ versus T showed a maximum followed by a shoulder, indicating some de-coupling of two relaxations, one of them undoubtedly related to isophorone cycle, not present in any of the networks studied.

Mechanical properties

In Figure 8 it can be observed that Young's modulus is related to the area under the β relaxation peak. This behavior was observed by Won et al.[36] on a series of networks based on DGEBA/IPD curing agent and trimethylcyclohexilamine (TMCA) as a chain extender. These authors show that the tensile moduli at room temperature decrease when the crosslinking density increases. The peak area of the β relaxation was found to decrease when the crosslinking density decreases. This has been considered a typical case of internal antiplasticization, which is defined by an increase of the Young's modulus, and at the same time a decrease in the glass transition temperature and in the amplitude of the β relaxation. However in the formulations used in this study was not observed the decrease in the glass transition temper-

TABLE V
Mechanical Characterization

Networks	E (GPa)	σ_r (MPa)	ε_r (%)	E_Y (GPa)	σ_Y (MPa)	ε_Y (%)
DGEBA/EDA	–	–	–	2.64 ± 0.09	110 ± 4.0	6.9 ± 1.1
DGEBA/DETA	2.55 ± 0.11	54 ± 2	4.7 ± 0.4	2.61 ± 0.22	108 ± 7.5	6.6 ± 1.5
DGEBA/TETA	2.42 ± 0.15	53 ± 2	4.8 ± 0.3	2.41 ± 0.04	111 ± 3.6	7.0 ± 1.8
DGEBA/TEPA	2.34 ± 0.13	54 ± 3	5.1 ± 0.1	2.48 ± 0.11	100 ± 2.7	6.7 ± 1.1
DGEBA/AEP	2.47 ± 0.15	56 ± 1	6.6 ± 0.4	2.44 ± 0.02	95 ± 0.5	7.3 ± 0.2
DGEBA/IPD	2.65 ± 0.05	58 ± 6	4.7 ± 1.0	2.85 ± 0.03	123 ± 0.6	7.8 ± 0.2

E = Young's modulus, σ_r, ε_r = stress, strain at the break, E_y = Flexural modulus, σ_y, ε_y = stress, strain at the maximum.

ature. Thus, this effect is particular of T_β and is not present in the T_g at all for the studied systems.

The results related to tensile and flexural tests are reported in Table V and the flexural stress–strain curves obtained by three point bending test are given in Figure 9. For all networks studied in this work, the Young's moduli are in the range commonly found for epoxy/amine networks.[15,36–39]

During the tensile tests, the epoxy network under study is broken without no yielding considering the yielding is taken as the strength. For networks based on the series of ethyleneamines, DETA showed the highest modulus, while the lowest modulus is observed for the network based on TEPA. These results are according to the fact that an increase of functionality induces an increase in crosslinking density and therefore the modulus decreases. The network based on AEP has a similar tensile value to that of the DGEBA/TETA system, but its flexural behavior gives the best values taken into consideration the high value of the flexural strain ($\varepsilon_y = 7.3\%$) and the lower value of the flexural stress ($\sigma_y = 95$ MPa). This is indicating the more flexibility of the network. However, IPD network present the worst tensile and flexural behavior when compared with AEP network.

The behavior of the cyclic series (AEP and IPD) is similar to the linear one because IPD has a functionality higher than of AEP, but IPD presents the higher value of all of them. This is true for tensile and flexural tests. It is interesting in Figure 9 to note the plastic behavior of the AEP network. This behavior is only observed for the AEP network and confirms the more flexibility of the network.

The results concerning the fracture toughness are reported in Table VI. The values obtained (K_{IC} and G_{IC}) for the networks on the series of ethyleneamines
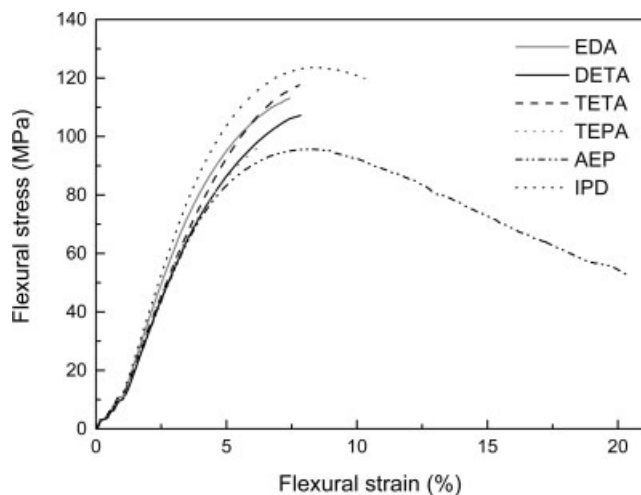
TABLE VI
Toughness Properties

Networks	K_{IC} (MPa m$^{1/2}$)	G_{IC} (kJ m^{-2})
DGEBA/DETA	0.73 ± 0.18	0.18
DGEBA/TETA	0.72 ± 0.03	0.18
DGEBA/TEPA	0.70 ± 0.17	0.18
DGEBA/AEP	0.91 ± 0.16	0.29
DGEBA/IPD	0.78 ± 0.11	0.20

are close to the values generally observed for epoxy/amine networks.[15,39] In this case a similar value of K_{IC} was obtained for all these networks. The network based on the AEP exhibits the highest value of K_{IC} and G_{IC} for all the systems. Furthermore, the network based on IPD has a higher value than any of the linear series of ethyleneamines.[37] Thus, both cyclic amines improve the fracture toughness.

The fracture toughness of a material depends on its ability to absorb or dissipate energy, which requires chain mobility. It seems that cyclic amines offer a more local flexibility to dissipate energy.

CONCLUSIONS

We have studied two series of epoxy/amine networks cured with aliphatic linear and cyclic amines differing by their chemical structure.

Functionality rules the behavior by increasing the crosslinking density in both series increasing T_g and decreasing the tensile and E_y.

Besides, the Young's modulus E is linked to the amplitude of the β relaxation for the series of linear ethyleneamines.

Cyclic series presents an extremely different behavior. IPD network was the worst respect to tensile and flexural behavior while AEP and IPD networks presented the best fracture toughness. In general, AEP network resulted the best of all for practical mechanical purposes.

Figure 9 The flexural stress–strain curves obtained by three-point bending test for the various networks.

References

1. Sultan, J. N.; McGarry, F. J. Polym Eng Sci 1973, 13, 29.
2. Visconti, S.; Marchessault, R. H. Macromolecules 1974, 7, 913.
3. Hedrick, J. H.; Yilgor, I.; Wilkens, G. L.; McGrath, J. E. Polym Bull 1985, 13, 201.
4. Bucknal, C. B.; Gilbert, A. H. Polymer 1989, 30, 213.
5. Dow Chemical. U.S. Pat. 4,594,291 (1986).
6. Misra, S. C.; Manson, J. A.; Sperling, L. H. Am Chem Soc 1979, 114, 137.
7. Lemay, J. D.; Swetlin, B. J.; Kelley, F. N. Am Chem Soc 1984, 243, 165.
8. Choy, I. C.; Plazek, D. J. J Polym Sci Part B: Polym Phys 1986, 24, 1303.
9. Hodges, W. T.; St. Clair, T. L.; Pratt, T. R.; Ficklin, R. SAMPE Q 1985, 17, 21.
10. Varma, I. F.; Satya-Bhama, P. V. J Compos Mater 1986, 20, 410.
11. Delvigs, P. Polym Compos 1986, 7, 101.

12. Grillet, A. C.; Galy, J.; Pascault, J. P.; Bardin, I. Polymer 1989, 30, 2094.
13. Bondi, A. J Phys Chem 1964, 68, 441.
14. Bellenger, V.; Dhaoui, W.; Verdu, J. J Appl Polym Sci 1987, 33, 2467.
15. Pascault, J. P.; Sautereau, H.; Verdu, J.; Williams, R. J. J. Thermosetting Polymers; Marcel Dekker: New York, 2002; Chapter 10–12.
16. Galy, J.; Sabra, A.; Pascault, J. P. Polym Eng Sci 1986 26, 1514.
17. Vallo, C. I.; Frontini, P. M.; Williams, R. J. J Polym Sci Part B: Polym Phys 1991, 29, 1503.
18. Eloundou, J. P.; Feve, M.; Harran, D.; Pascault, J. P. Die Angwdte Makromol Chem 1995, 230, 13.
19. Klute, C. H.; Viehmann, W. J Appl Polym Sci 1961, 5, 86.
20. Horie, K.; Hiura, H.; Sawada, M.; Mita, I.; Kambe, H. J Polym Sci Part A-1: Polym Chem 1970, 8, 1357.
21. Rozenberg, B. A. Kinetics, In Epoxy Resins and Composites II; Dušek, K., Ed.; Springer-Verlag: Berlin, 1986; p 115.
22. Gillham, J. K. J Appl Polym Sci 1973, 17, 2067.
23. Ochi, M.; Yoshizumi, M.; Shimbo, M. J Polym Sci Part B: Polym Phys 1987, 25, 1817.
24. Ochi, M.; Iesako, H.; Nakajima, S. J Polym Sci Polym Phys Edn 1986, 24, 251.
25. Ochi, M.; Shimbo, M.; Saga, M.; Takashima, N. J Polym Sci Part B: Polym Phys 1986, 24, 2185.
26. Heux, L.; Halary, L.; Lauprêtre, F.; Monnerie, L. Polymer 1997, 38, 1767.
27. Struik, L. C. E. Polymer 1987, 28, 57.
28. Ochi, M.; Iesako, H.; Shimbo, M. Polymer 1985, 26, 457.
29. Takahama, T.; Geil P. H. J Polym Sci Polym Phys Edn 1982, 20, 1979.
30. Ochi, M.; Okazaki, M.; Shimbo, M. J Polym Sci Polym Phys Edn 1982, 20, 689.
31. Chang, T. D.; Carr, S. H.; Brittain, J. O. Polym Eng Sci 1982, 22, 1205.
32. Williams, J. G. J Appl Polym Sci 1979, 23, 3433.
33. Grillet, A. C.; Galy, J.; Gérard, J. F.; Pascault, J. P. Polymer 1991, 32, 1885.
34. Dammond, F. R.; Kwei, T. K. J PolymSci 1967, 5, 761.
35. Takahama, T.; Geil, P. H. J Polym Sci Polym Phys Edn 1972, 13, 450.
36. Won, Y. G.; Galy, J.; Gérard, J. F.; Pascaultd, J. P.; Bellenger, V.; Verdu, J. Polymer 1990, 31, 1787.
37. Urbaczewski-Espuche, E.; Galy, J.; Gérad, J. F.; Pascaultd, J. P.; Sautereau, H. Polym Eng Sci 1991, 31, 1572.
38. Franco, M; Mondragon, I; Bucknall, C. B. J Appl Polym Sci 1999, 72, 427.
39. Crawford, E. D.; Lesser, A. J. Polym Eng Sci 1999, 39, 385.